On-orbit calibration of the Ultraviolet/Optical Telescope (UVOT) on Swift: Part 2

A. A. Breeveld[1], T. S. Poole[1], C. H. James[1], A. J. Blustin[1], S. R. Rosen[1], W. Landsman[3], P. Boyd[3], C. Gronwall[2], S. Holland[3], S. D. Hunsberger[2], M. Ivanushkina[2], K. O. Mason[1], K. McGowan[1], M. de Pasquale[1], P. W. A. Roming[2], M. Still[3]
[1]Mullard Space Science Laboratory, UCL, Holmbury St. Mary, Dorking, Surrey, RH5 6NT, UK
[2]Pennsylvania State University, 525 Davey Lab, University Park, PA 16802, USA
[3]NASA/Goddard Space Flight Center, Code 660.1, Greenbelt, MD 20771, USA

1. ABSTRACT

The Ultraviolet and Optical telescope (UVOT) on board the SWIFT observatory, plays an important part in the quest to understand gamma-ray bursts. As its name suggests, the UVOT obtains ultraviolet and optical data at high time resolution, with 7 broad band filters and 2 low resolution grisms.

This paper forms the second of a pair of papers presenting the initial on-board calibration of the UVOT. The first one (Part 1) deals with distortion, large and small scale sensitivity variations and the telescope point spread function.

In this paper we cover the following topics: the photometry of the broadband filters including colour transformations and linearity; the wavelength calibration and sensitivities of the grisms; time resolution and red leak.

2. INTRODUCTION

The UVOT makes an important contribution to the science of the SWIFT observatory by providing coverage of the central 17x17 arcmin field of view in the optical or UV band (range 170-600nm), at the same time as the XRT and BAT observations. The UVOT has a spatial scale of 0.5 arcsecs/pixel with a timing resolution of 11ms for the full field of view. Seven broad-band filters allow colour discrimination, and there are two grisms, one in the UV and one in the optical, to provide low resolution spectroscopy.

More detailed information about SWIFT may be found in Gehrels et al. (2005)[1] and about UVOT in Roming et al. (2005)[2]. The ground based calibration is described in Mason et al (2004)[3].

Substantial progress has already been made on the calibration so that positions, magnitudes and fluxes can be measured with confidence. This paper forms the second of a pair of papers presenting the initial on-board calibration of the UVOT. The first one (Part 1; in these proceedings) deals with distortion, large and small scale sensitivity variations and the telescope point spread function. This paper gives a summary of different aspects of the UVOT calibration in the following sections: (i) Photometry, including colour transformations, linearity and counts to flux conversions, (ii) Grism calibration, including wavelength and sensitivity (iii) Timing and (iv) Red leak.

3. PHOTOMETRY

Table 1 gives a list of the UVOT filters, including the grisms, with their approximate wavelength ranges (FWHM) and in-orbit zero points. The UV grism range has to be artificially cut off at 360 to avoid contamination with 2nd order light. To measure the on-board response of the UVOT, we observed photometric standard stars. Slightly different methods for calculating the zero points for the optical and ultraviolet filters were used because the optical zero points need to match a standard magnitude system, but for the ultraviolet, although instrumental magnitudes are given, the emphasis is on measuring fluxes.

UV, X-Ray, and Gamma-Ray Space Instrumentation for Astronomy XIV
edited by Oswald H. W. Siegmund, Proc. of SPIE Vol. 5898
58981E, (2005) · 0277-786X/05/$15 · doi: 10.1117/12.616817

Filter	Waveband (nm)	Zero point (mag)	Error on zero point (mag)	Dispersion (nm/pix)
V	510 – 580	17.88	0.09	
B	390 – 490	19.16	0.12	
U	300 – 390	18.38	0.23	
UVW1	220 – 300	17.69	0.02	
UVM2	200 – 250	17.29	0.23	
UVW2	170 – 230	17.77	0.02	
White	170 – 590	19.78	0.02	
Visible grism	290 – 650			0.62
UV grism	180 – 360			0.39

Table 1 The wavelength ranges and zero points of the UVOT filters. Dispersions are given for the UVOT grisms.

3.1. Optical Zero Points

We took observations of 15 Landolt stars[4] , 4 white dwarf stars (WD1657+343, WD 0947+857, WD1026+453 and WD1121+ 145) and 2 Oke Standard stars (SA95-42 and G24-9) with known Johnson UBV magnitudes. All observations were reprocessed using the latest SWIFT Calibration Database (CALDB) teldef file[5] and software[9]. Raw count rates for each star were extracted using an aperture radius of 12 pixels (6 arcsec), and then corrected for dead time and coincidence loss using the equations given in 3.5. Optical zero points were then calculated using:

$$Z_{pt} = M_{std} + 2.5\log(C_{obs}) \quad (1)$$

where Z_{pt} is the optical zero point, M_{std} is the standard V, B or U magnitude of the star, and C_{obs} is the corrected, observed count rate of the star in the V, B or U filters. Figure 1 shows the data used to calculate the zero points. Z_{pt} is found where the fitted line crosses the y-axis. The error bars in the plots are propagated from the measurement error in extracting the raw, observed count rate. Taking colour terms into account for these observations showed that there was a very small colour dependence, therefore we have not taken colour into account for the preliminary optical zero points reported here.

3.2. Ultraviolet and White Zero Points

We took observations of the 4 faint white dwarf stars (see 3.1) with known ultraviolet spectra, although for some stars the spectra did not cover the whole range of wavelengths required, so a subset had to be used for some filters. We extracted the raw count rates for each star using an aperture radius of 24 pixels (12 arcsec), and then corrected for coincidence loss (see 3.5). For the white filter an aperture radius of 12 pixels (6 arcsecs) was used.

Magnitude systems are not widely used in the ultraviolet so we have chosen to calculate the zero points by standardising the count rates to a Vega spectrum, using the ground based effective areas[6], re-normalised to fit the in-orbit count rates (see 3.3). Ultraviolet and white zero points for each filter were then calculated using:

$$Z_{pt} = M_{vega} + 2.5\log(C_{vega\_corr}) \quad (2)$$

where Z_{pt} is the zero point, M_{vega} is the standard Vega magnitude for each ultraviolet or white filter (0.025), and C_{veg_corr} is the Vega count rate, corrected for in-flight response.

The final zero point for each filter was calculated by averaging over all the observations in that filter. Figure 2 shows the measurements. The error bars in the plots are propagated from the measurement error in extracting the raw count rate.

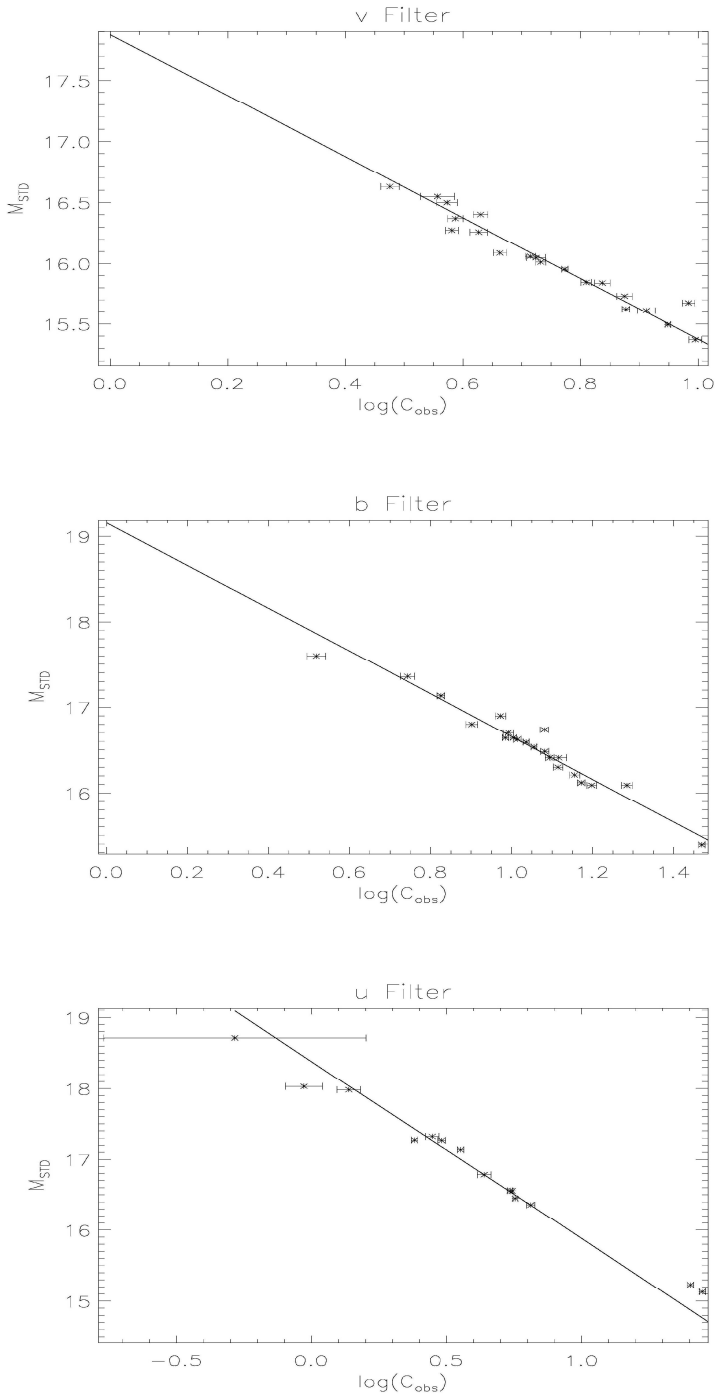

Figure 1 Measuring the optical zero points using standard stars.

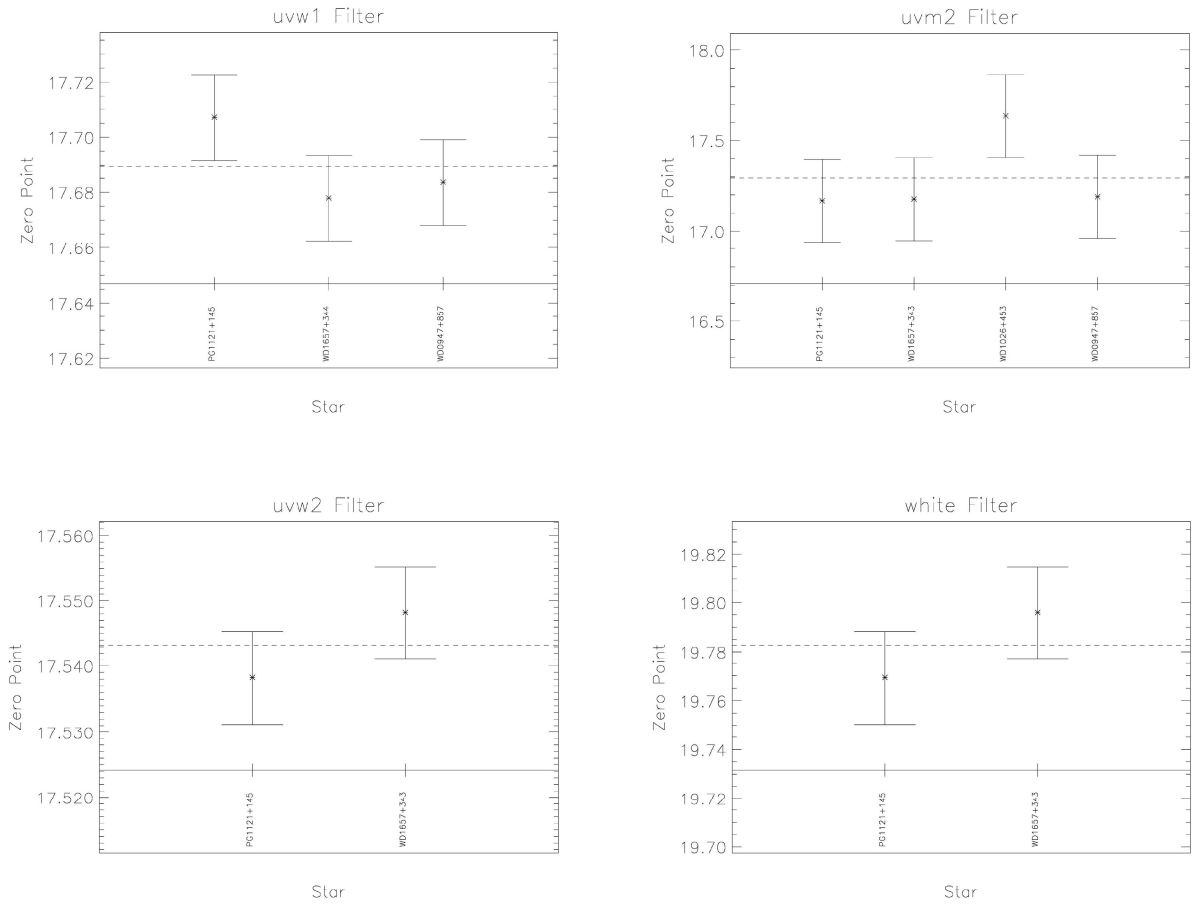

Figure 2 Zero point measurements for UV and White filters. The identities of the stars are indicated.

3.3. Effective Areas

The effective area curve is calculated in units of cm^2. If the effective area is divided by the aperture of the telescope (661 cm^2), then the result is the fraction of photons passing through the aperture that are successfully recorded by the detector. The four main components defining effective area are aperture size, mirror reflectivity, filter transmission and detector efficiency. Effective area is therefore dependent upon both wavelength and the specific filter in use.

The in-orbit effective areas are based on those calculated pre-launch using the manufacturers filter transmission curves and ground based calibration[3,6]. They are adapted for flight by re-normalising to measured count rates, using the white dwarfs described in 3.1. The ground-based effective area curves were only measured down to 188nm and therefore they have been extrapolated to 160nm to match the expected telescope limits. All observations were reprocessed using the latest CALDB teldef file[5]. Where multiple observations were taken, images were spatially corrected and then co-added. The observed count rates were obtained using 12 pixel (6 arcsec) aperture radii for optical and white filters and a 24 pixel (12 arcsec) radii for ultraviolet filters. All count rates were then corrected for coincidence loss.

We obtained the expected count rates for the white dwarfs in each filter by convolving the known spectrum of each source with the ground based effective area curves[6].

Ratios of observed to expected count rates are given in Table 2. These ratios were used to modify the ground-based effective area curves for in-orbit use.

Figure 3 shows the comparison between the in-orbit effective area curves (solid lines), and the ground based effective area curves (dashed lines). The in-orbit white filter effective area curve was calculated by multiplying each filter point by the appropriate average filter ratio. This method for the white filter has been double checked by obtaining count rates in all filters for a set of random stars, converting these to flux (see 3.4) and folding the resulting spectrum through the in-orbit white filter effective area curve.

Filter	Average Count Rate Ratio
V	0.80±0.07
B	0.86±0.09
U	0.66±0.02
UVW1	0.64±0.01
UVM2	0.77±0.17
UVW2	0.86±0.01

Table 2 Ratio of in-flight to expected pre-flight count rates

3.4. Count Rate to Flux Conversion

Many people prefer not to use magnitudes, but require a flux measurement of their source at a particular wavelength for plotting in multi-wavelength Spectral Energy Distributions (SEDs). For broadband filters the translation from counts to flux depends on the spectrum of the source because counts are collected over a range of wavelengths. However, by modelling a wide range of spectral types we have found that the count to flux ratio does not vary by more than ~20%; the filters being narrow compared with the rate of change of the spectrum.

We have obtained a count rate to flux conversion for each filter in two ways; firstly by observation of well-known sources and secondly by convolving a spectrum of known flux (e.g. Vega) with the in-flight effective area curves. The four white dwarfs and Oke Standards mentioned in 3.1 are suitable for this calculation. Vega cannot be observed by UVOT because it is too bright.

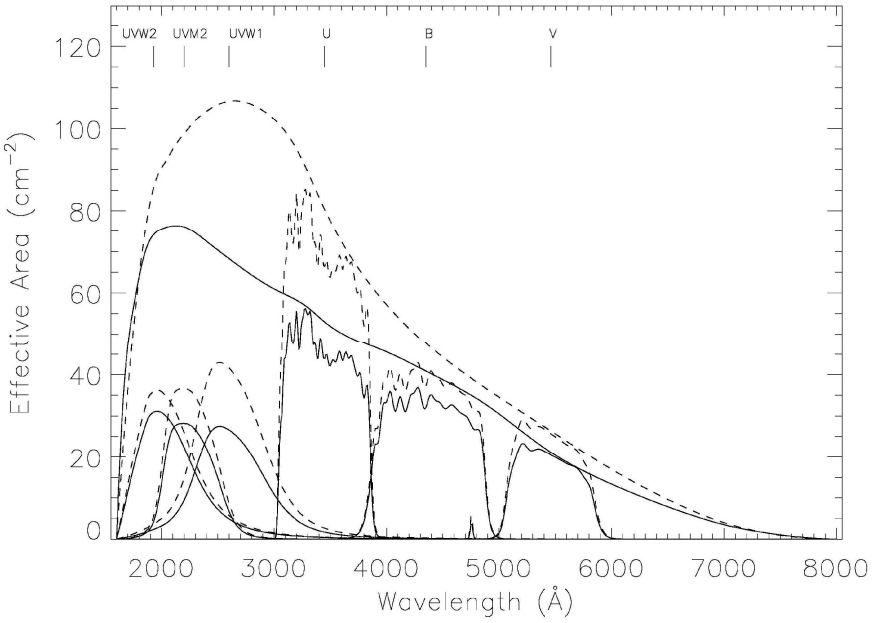

Figure 3 Effective area curves. Solid lines in-orbit; dashed lines ground-based curves. The midpoints of the 6 colour filters are indicated at the top of the plot. The white filter curve encloses the others.

There are several ways in which we could define the flux at a given wavelength. We have found the most reliable way is to fit a continuum to the known spectrum, and use interpolation to find a flux value at a given wavelength. This method has the advantage that it does not give weight to noise and spectral features. The effective filter wavelengths are given in Table 3.

The interpolated fluxes for WD1657+343 and Vega are plotted as stars in Figure 4. For Vega, the B filter effective wavelength lies over an absorption feature in the spectrum, but the interpolation has over-come this.

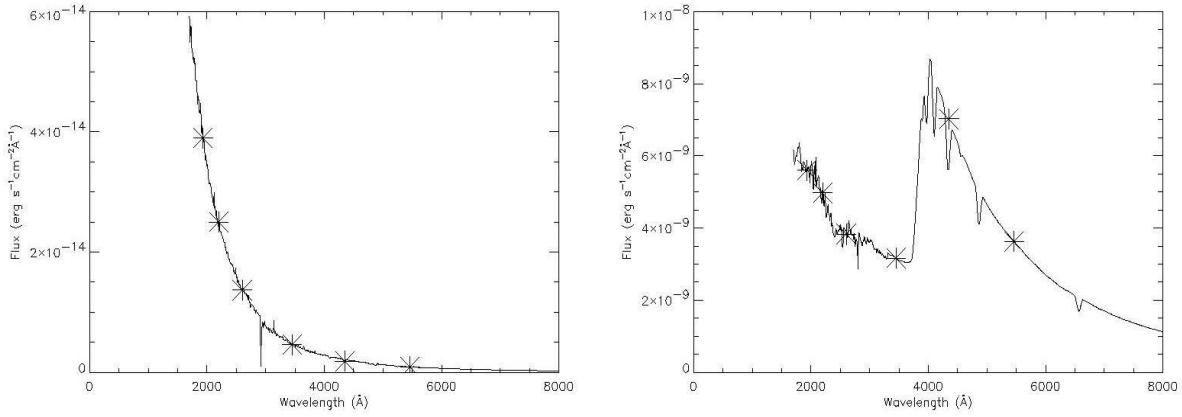

(a) **(b)**

Figure 4 – Spectra with flux values for each filter highlighted in magenta (a) WD1657+343, (b) Vega.

The count rate to flux conversion (ergs s^{-1} cm^2 $Å^{-1}$ cts^{-1}) was calculated using the seven different count rate values (six observed and one simulated) and the associated flux values. Table 3 shows the average count rate to flux conversion ratio (column 3) and the standard deviation of the average for each filter (column 4). To obtain the flux associated with a given count rate in a filter, multiply by the given ratio.

Filter	Wavelength (Å)	Ratio	Ratio Error
V	5460.0	2.236803E-16	1.211080E-17
B	4350.0	1.313720E-16	1.429925E-17
U	3450.0	1.485137E-16	6.016375E-18
UVW1	2600.0	3.520731E-16	6.909226E-18
UVM2	2200.0	6.886721E-16	9.632383E-17
UVW2	1930.0	6.039047E-16	4.207662E-17

Table 3 - Average count rate to flux conversion ratio results.

3.5. Coincidence loss

The UVOT detectors suffer from coincidence losses at high count rates, when more than one photon strikes the same area of the CCD (the effective coincidence area) during a single readout period. For a full frame the readout takes ~11ms, therefore photons will start to be lost for count rates above about 10c/s for a point source. The correction for coincidence loss for a point source is given by equation (3):

$$C_{theory} = \frac{-\ln(1 - C_{raw} ft)}{ft(1 - df)} \tag{3}$$

where C_{theory} is the incident count rate (i.e. the measured count rate corrected for coincidence loss), C_{raw} is the raw observed count rate, *ft* is the frame time, and *df* is the deadtime fraction. For a full frame readout *ft* = 0.011088s and *df* = 0.0155844.

Since all the photons do not arrive at exactly the same point on the CCD a further correction to this equation needs to be determined empirically. An empirical correction for coincidence loss was determined from ground-based calibrations and is included in the current pipeline and given in (4) and (5). The accuracy of this calibration can be assessed from Figure 5, in which B photometry from a UVOT image of the Small Magellanic Cloud is compared, with and without a coincidence loss correction, to published photometry from the Magellanic Cloud Photometric Survey[7]. There is still a small under correction for stars with B < 13.5, but at fainter magnitudes the ground-based calibration performs well.

$$f(x) = 1.0 + 0.2966x - 0.492x^2 - 0.4183x^3 + 0.2668x^4 \quad (4)$$

where $x = C_{raw} ft$

Then the full coincidence loss corrected incident count rate is given by:

$$C_{emp} = C_{theory} f(x) \quad (5)$$

Further refinement of the coincidence loss correction will be determined from observations of a photometric field using a hardware window with double and four times the nominal frame rate (with half and quarter the field of view, respectively).

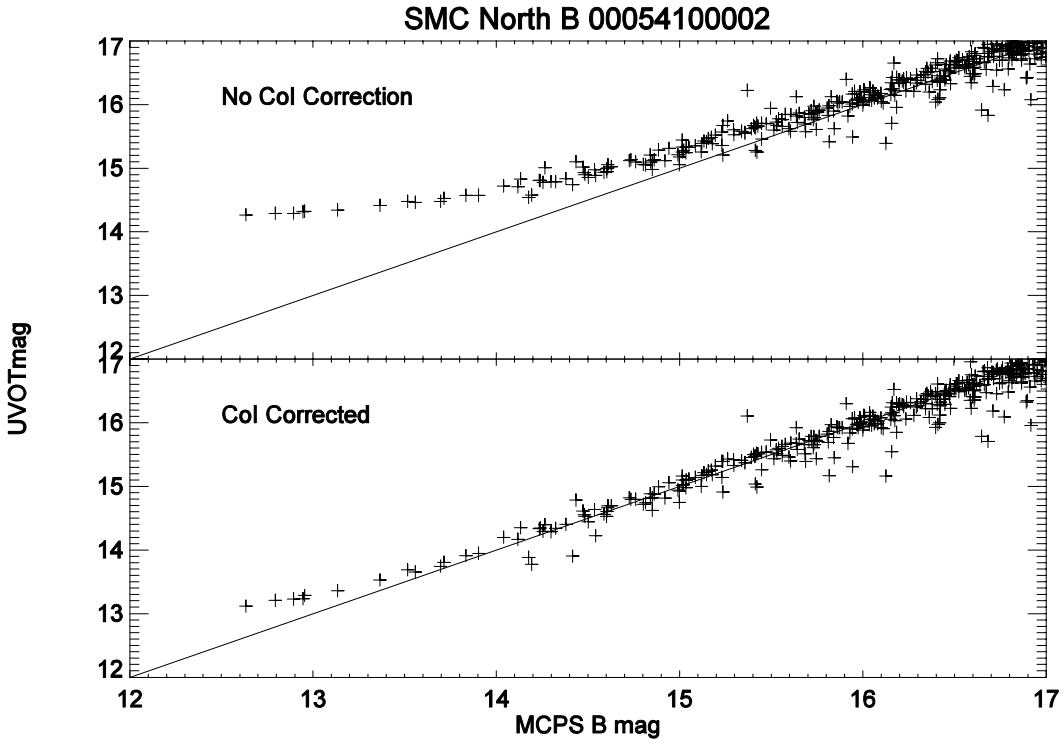

Figure 5 Coincidence loss correction

3.6. Colour transformation

Although the UVOT optical filters are based on the Johnson standards, they are not identical to them and therefore colour transformations need to be derived so that UVOT colours can be adjusted to the standard photometric system. Pre-launch, colour transformations were estimated by convolving model stellar spectra with the UVOT filter response curves,

and then comparing the resulting colours with those obtained observationally from a calibration field. In order to derive transformations based upon UVOT performance in orbit, we carried out a series of observations of a field in the Small Magellanic Cloud (SMC). The target field was chosen on the basis of having a large number of blue stars, since UVOT is most sensitive at the blue end of the spectrum. Images were obtained in all six optical and UV broad band filters.

A set of source regions was created using the Magellanic Clouds Photometric Survey[7] (see Figure 6). The resulting region file was filtered to remove unsuitable sources**;** these were defined as those falling outside the bounds of the images, those with extraction regions overlapping with nearby stars, regions close to bright stars and therefore affected by coincidence loss/mod-8 pattern noise, and regions in an area of high background at the centre of the field. Initially, work has concentrated on the three optical filters. The region file was used to perform aperture photometry on the sources in the U, B and V images with the *Autophotom* routine[8] (one of the *Starlink* tools). Since the field is extremely crowded, the normal 6 arcsec radius aperture is too large and therefore a 3 arcsec radius aperture was used. An aperture correction was applied to the source counts before conversion to magnitude using the in-orbit zero points.

The resulting source list with magnitudes was then cross-correlated with the original catalogue source list. B-V and U-B colours were calculated for both measured and catalogue magnitudes and, in each case, the sets of colours were plotted against each other. There is an approximately linear relationship between UVOT and catalogue colours, and current work focuses on reducing the spread in the measured magnitude to constrain the relationship as well as possible.

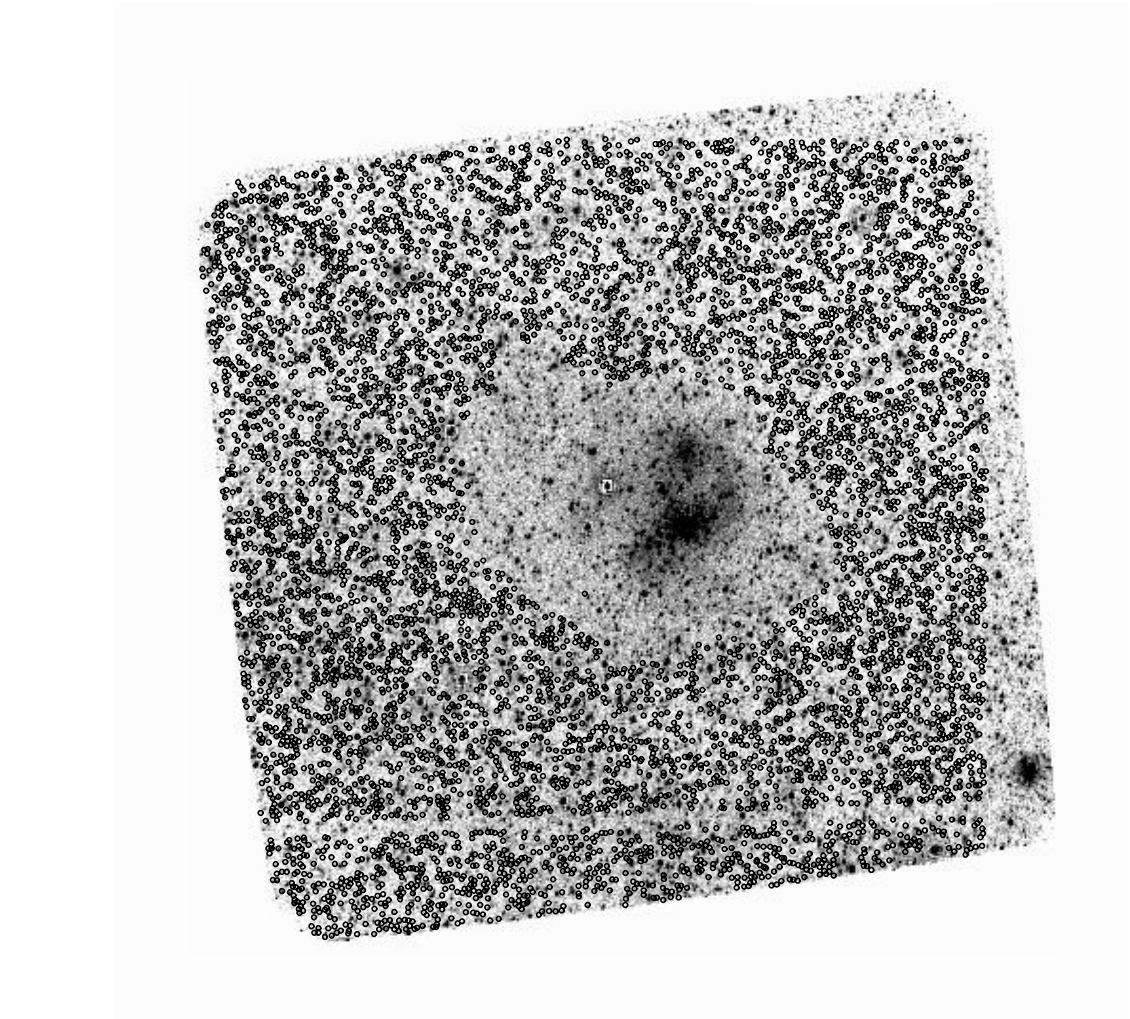

Figure 6 V band colour transformation field with photometry apertures superimposed (small black circles).

4. GRISM CALIBRATION

Figure 7 shows a slice of a visible grism image plus the extracted spectrum from UVOT. For each source the grism disperses the zeroth order light (the blob on the left of the image) and first order dispersed light (the streak on the right of the image), in opposite directions. A special set of CALDB grism teldef files (one for each grism; V or UV) for the positions of the zeroth order spectra have been produced to help identify the spectra associated with targets of interest, by giving the sky coordinates of the centre of the field of view, the plate scale and rotation.

First order spectra can suffer from overlap with zeroth order spectra from other sources. In order to reduce this possibility the filter wheel can be "clocked" further round to reduce the number of sources in the grism field of view. We expect the wavelength and sensitivity calibrations to change slightly with the clocked positions and therefore intend to release separate CALDB products for "nominal" and "clocked" positions. We are also checking whether vignetting will require extra products for sources some distance away from the boresight.

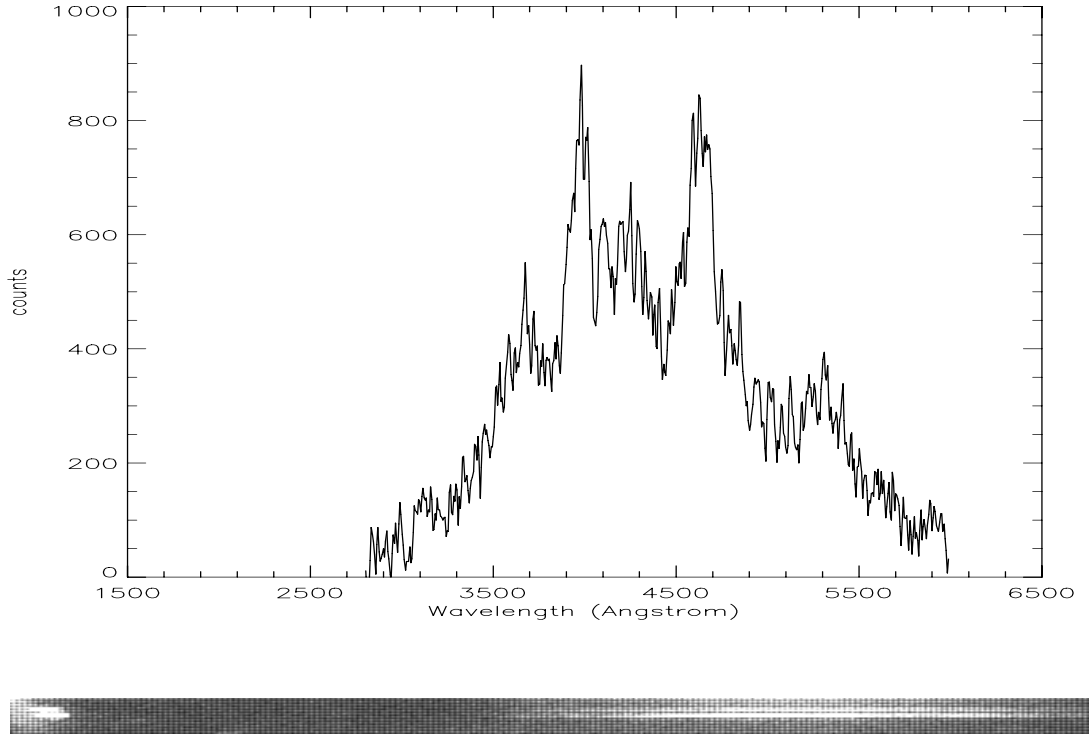

Figure 7 Visible Grism 2d image and extracted spectrum from SN2005am. The SN lies close to the galaxy NGC 2811 and close to another object. It is the lower spectrum in the image.

4.1. Wavelength calibration

The wavelength scale is expressed as a polynomial equation in terms of the distance from the anchor point, along the spectrum in the dispersion direction. The anchor point is defined as the centroid of 8x8 sub-pixel area centred on the maximum of the zeroth order spectrum. The advantages of this method are that it is repeatable and simple to apply. It does not take into account the variation in the position of the maximum with spectral type, but this effect is found to be small compared with other errors. Observations of spectrophotometric standard stars that exhibit multiple emission lines at well-defined wavelengths within the waveband of the grisms are used to map dispersion position to wavelength.

It may be that the grism equation depends not only on the grism filter (UV or V), but also on the clocked position of the filter wheel and the location of the object on the detector face. Hence there are separate grism equation products for each grism filter, for spectra associated with targets at the boresight and four offset positions (boresight +/- 3arc seconds) and with the filter wheel in both the default and clocked positions; a total of twenty products. Work is still in progress on revising these calibration products from in-flight measurements, however the ground based calibration[3] can already be used with reasonable accuracy.

4.2. Sensitivity with wavelength

We derive the calibrated flux scale by defining the grism sensitivity function (GSF).

$$GSF(\lambda) = R_{std}(\lambda) / P_{cat}(\lambda) \tag{6}$$

where $R_{std}(\lambda)$ is the observed counts.s^{-1}.Angstrom^{-1}of a standard star and $P_{cat}(\lambda)$ is the catalogue flux (erg s^{-1} cm^{-2} Angstrom $^{-1}$) of the same standard star at wavelength (λ) (Angstrom) converted to a photon count through using the relationship:

$$Flux(\lambda) = photoncount(\lambda) \times E(\lambda) \tag{7}$$

where $E(\lambda)$ is the energy of the photon at wavelength (λ), i.e. E = hc/λ.
The GSF is expressed in units of cm^2.

The observed flux of an arbitrary star F_{arb} is obtained by

$$F_{arb}(\lambda) = R_{arb}(\lambda) E(\lambda) / GSF(\lambda) \tag{8}$$

where $R_{arb}(\lambda)$ is the observed count s^{-1} Angstrom^{-1} at wavelength, λ of the arbitrary star. It is expressed in units of erg s^{-1} cm^{-2} Angstrom $^{-1}$.

4.2.1. Observations

We have chosen as our calibration sources, spectrophotometric standard stars which are continuum rich and spectral line poor, lie in sparse star fields and are sufficiently faint to give less than 10% co-incidence loss for the first order spectrum. Calibration observations for the UV-GSF have included the white dwarfs WD0320-539, WD1057+719 and for the V-GSF, the white dwarfs GD50 and GD153.

To promote consistency between the calibration and scientific analyses we extract the grism spectra using the UVOT specific software[9] on the raw data starting with *uvotbadpixels,* followed by *swiftxform* and finally *uvotimgrism.* In *swiftxform* we use the *area* method with bitpix set to *-32* and convert to *DET* co-ordinates. We measure the angle of rotation and the position of the anchor point (mm) prior to rotating the spectrum about the anchor-point in uvotimgrism which also performs background subtraction and extraction of the 1st order spectrum.

The catalogue and observed spectra are rebinned into 40 Å steps and, where multiple exposures of the same target exist, an average spectrum is calculated. Anomalies (unwanted spectral lines) are removed using linear interpolations, prior to the calculation of a target specific GSF. An average GSF is calculated from multiple target GSFs. We check the veracity of the final GSF by applying it to UVOT data of a non-participating spectrophotometric standard star using equation (8). We use IDL procedures to perform all of the GSF analysis. The data extraction and analysis for the UV and Visible GSF in the default position are still in progress.

5. TIMING

The time resolution of UVOT event mode data is defined by the frame time (~11ms in full frame mode), potentially providing high time-resolution data for bright sources. The absolute and relative timing accuracy of UVOT data is therefore important for burst analysis (e.g. for comparing data to other instruments) and for data from rapidly variable sources such as pulsars etc.

The choice of targets to assess the UVOT timing accuracy was complicated by the brightness restrictions ($15<B<18$ due to the need to minimize coincidence loss effects while achieving adequate signal) and the requirement that they exhibit stable fiducial features with accurately predictable timings. As first order checks, the AM Herculis binaries, UZ For and HU Aqr were observed by both UVOT (in full-frame mode through the U filter) and, contemporaneously, with the SAAO 1.9m telescope/UCT photopolarimeter (data taken and analysed by S. Potter).

Two eclipses of UZ For were observed. The epochs of eclipse centre could be determined, for both the UVOT and ground data, to an accuracy of approximately 1s. The UVOT and ground-measured eclipses times are consistent for both eclipses, with a temporal displacement of less than about 1.5s. The analysis of a larger set of HU Aqr data is ongoing.

Tighter constraints may be achievable (~0.1s) from observations of the 7.7s pulsar, 4U1626-67. This target, however, was too faint for the 1.9m telescope - ground based coverage is essential as, despite its highly constrained rotation period, previous observations can not be extrapolated to the current epoch with adequate accuracy.

We are seeking to exploit the 8m SAAO SALT to re-observe HU Aqr and also 4U1626-67 to tighten constraints on the absolute timing accuracy of UVOT.

6. RED LEAK

Any transmission through the UV filters of visible light is known as a red leak. For an object with a predominantly optical spectrum, the percentage of light leaked into the UV filters could be significant compared with real UV counts. To measure the red leak we have observed highly reddened stars and late-type stars which should produce virtually no UV. The counts obtained in the UV filters are compared with modelled data and also with those obtained in the optical filters to see whether any correlation can be found. Any red leak at longer wavelengths than 700nm will not be observed due to the limits of the detector window transmission.

Many M-type stars were selected and have been observed in the 6 broad band filters. They were chosen to give an expected count rate below 90c/s in the optical filters (which is the maximum for which we can accurately correct coincidence loss). These data are still being analysed.

7. CONCLUSIONS

A thorough calibration of any instrument is vital if the science is to be believed. Although we have made great strides in the calibration of the UVOT already, much remains to be done. Over the next few months we expect further improvement of the photometry when more spectrophotometric standard stars have been observed. The colour transformations, co-incidence loss and grism calibrations are also expected to be delivered. Other calibrations will be updated and changes monitored with further calibration observations and continued analysis.

8. ACKNOWLEDGEMENTS

This work is supported at MSSL by funding from PPARC and from PSU by NASA's Office of Space Science through grant NAG5-8401.

9. REFERENCES

1. Gehrels N. et al., ApJ 611 p1005, 2005
2. Roming P.W.A., Kennedy T.E., Mason K.O., Nousek J.A., Ahr L., Bingham R.E., Broos P.S., Carter M.J., Hancock B.K., Huckle H.E., Hunsberger S.D., Kawakami H, Killough R., Koch T.S., McLelland M.K., Smith K., Smith P.J.,

Soto J.C., Boyd P.T., Breeveld A.A., Holland S.T., Ivanushkina M., Pryzby M.S., Still M.D., Stock J., "The Swift Ultra-Violet/Optical Telescope", Accepted for publication in SSRev Feb 2005.
3. Mason K.O., Breeveld A.A., Hunsberger S., James C., Kennedy T, Roming P., Stock J., Proc. SPIE vol5165, pp277-286, Feb 2004
4. Landolt A. U., Astron. J. Vol 104 (1), p.340, July 1992
5. HEASARC's calibration database (CALDB) system stores and indexes datasets associated with the calibration of high energy astronomical instrumentation. The system can be accessed by users and software alike to determine which calibration datasets are available, and which should be used for data reduction and analysis. Swift caldb front page: http://heasarc.gsfc.nasa.gov/docs/heasarc/caldb/swift/
6. Roming, P., "Swift UVOT Instrument Science Report – Effective Area," PSU Documentation # SWIFT-UVOT-204-R01
7. Zaritsky et al. 2002, AJ 123, 855
8. Eaton, N., Draper, P. W. & Allan, A. 2002, Starlink User Note 45, Rutherford Appleton Laboratory (http://www.starlink.rl.ac.uk/star/docs/sun45.htx/sun45.html)
9. The Swift software is part of HEASoft, "A Unified Release of the FTOOLS and XANADU Software Packages". The current version of HEAsoft is 6.0. Web address: http://heasarc.gsfc.nasa.gov/docs/software/lheasoft/